

1 Supplementary Information: A 3D-integrated
2 BiCMOS-silicon photonics high-speed receiver
3 realized using micro-transfer printing

Ye Gu^{1*†}, He Li^{2*†}, Tinus Pannier^{1†}, Shengpu Niu¹,
 Patrick Heise^{3,4}, Christian Mai³, Prasanna Ramaswamy⁵,
 Alex Farrell⁵, Alin Fecioru⁵, Antonio Jose Trindade⁵,
 Ruggero Loi⁵, Nishant Singh¹, Senbiao Qin², Biwei Pan²,
 Jing Zhang², Johanna Rimböck⁶, Kristof Dhaenens⁷,
 Toon De Baere⁷, Geert Van Steenberge⁷, Dieter Bode⁸,
 Dimitrios Velenis⁸, Guy Lepage⁸, Neha Singh⁸,
 Joris Van Campenhout⁸, Xin Yin¹, Günther Roelkens^{2*},
 Peter Ossieur^{1*}

¹³ ¹IDLab, INTEC, Ghent University – imec, Ghent, 9052, Belgium.

14 ²Photonics Research Group, INTEC, Ghent University – imec, Ghent,
15 9052, Belgium.

³IHP- Leibniz-Institut für innovative Mikroelektronik, Frankfurt (Oder), Germany.

⁵ X-Celeprint Ltd., Lee Maltings, Dyke Parade, Cork, Ireland.

⁶ EV Group, E. Thallner GmbH, St. Florian am Inn, Austria.

22 ⁷Center for Microsystems Technology (CMST), INTEC, imec – Ghent
23 University, Ghent, 9052, Belgium.

⁸imec, Kapeldreef 75, Leuven, 3001, Belgium.

*Corresponding author(s). E-mail(s): Ye.Gu@ugent.be; He.Li@ugent.be;

Gunther.Roelkens@ugent.be; Peter.Ossieur@imec.be;

Contributing authors: Tinus.Pannier@ugent.be;

[†]These authors contributed equally to this work.

29 1 Transimpedance amplifier chiplet

30 The simplified schematic of the transimpedance amplifier (TIA) chiplet is shown in
 31 Fig. 1. The TIA input stage (TIS) utilizes a typical shunt feedback structure to convert
 32 the AC current signal of the PD into a voltage signal. Two electrostatic discharge
 33 (ESD) diodes, with a total of 51 fF parasitic capacitance, are placed at the input
 34 of the TIS to protect the internal circuits. Q_1 serves to alleviate the Miller effect of
 35 the parasitic base-collector capacitor of Q_0 . A shunt inductor L_1 , with $25 \times 25 \mu\text{m}^2$
 36 area, is used to increase the phase margin of the TIA loop. The feedback resistor R_F ,
 37 implemented as NMOS transistors and a polysilicon resistor, can be adapted by digital
 38 bits to compensate for the process variation. M_1 in the input DC current cancellation
 39 (IDCC) is used to absorb the DC current of the PD and the DC current of R_F . C_1 is
 40 used to compensate for the IDCC loop and alleviate the baseline wander. $R1 = 4k\Omega$,
 41 placed close to the base of Q_2 , is used to prevent the parasitic capacitance of the
 42 IDCC from affecting the high-speed path. As $R_{Ref} = 6 \times R_{C0}$, the Q_0 collector current
 43 $I_{C,Q_0} \approx 6 \times I_{ref} = 5.4\text{mA}$, which impacts the overall bandwidth and input-referred
 44 noise current of the TIA. I_{ref} is designed to be tunable and controlled by digital
 45 registers. R_{Ref} and R_{C0} are placed close to each other in the layout for matching.

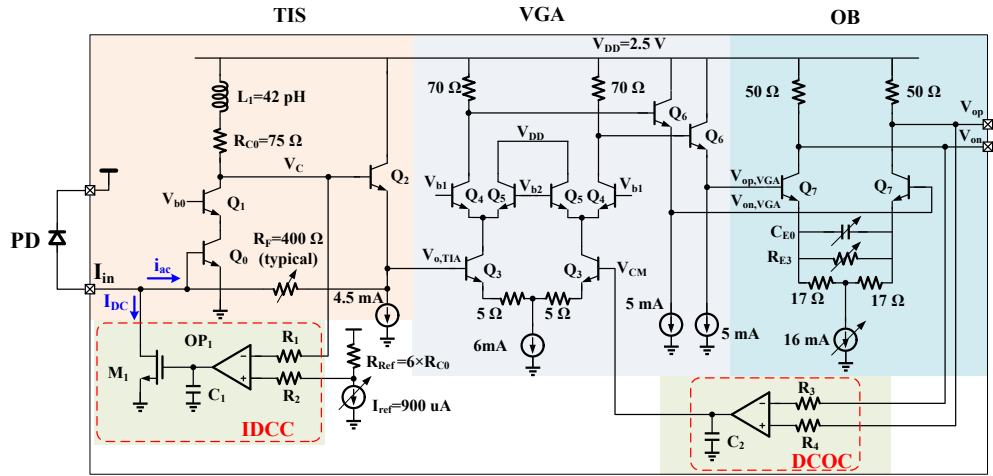


Fig. 1 Simplified schematic of the TIA chiplet.

46 The DC voltage at the input of the TIS is equal to one base-emitter forward bias
 47 voltage $V_{be,Q_0} \approx 0.75\text{V}$. The PD cathode bias voltage can be chosen to be the same
 48 as the main supply voltage of 2.5 V, so that the PD is reversely biased with a ~ 1.75
 49 V voltage difference.

50 The TIS is followed by the variable gain amplifier (VGA) stage, which also serves
 51 as a single-to-differential converter. One input of the VGA is connected to the output
 52 of the TIS, the other input is connected to a reference voltage generated by the DCOC.
 53 The gain of the VGA can be fine-tuned by changing V_{b1} and V_{b2} through digital bits.

54 Two $50\ \Omega$ resistors are used for impedance matching in the output buffer (OB)
55 stage. The OB stage has a tunable CTLE, realized by a tunable capacitor C_{E0} and a
56 tunable resistor R_{E3} . The R_{E3} is realized using NMOS transistors in the triode region,
57 whose resistance is programmable by tuning their gate voltages. The C_{E0} is realized
58 using PMOS varicaps, which can be fine-tuned by digital registers. The differential
59 outputs of the OB are also protected by ESD diodes.

60 2 Comparison with current state-of-the-art optical 61 receivers using different integrations

62 Table 1 shows the comparison with the state-of-the-art IMDD optical receivers using
63 different integration methods. This μ TP based optical receiver achieves the lowest
64 power consumption of 0.51 pJ/b and the smallest EIC area of 0.06 mm^2 .

Table 1 Comparison with current state-of-the-art PAM-4 optical receivers using different integrations.

ref.	Integration	EIC technology	Data rate (Gb/s)	R_T (dBΩ)	R (A/W)	Sens. @KP4 (dBm)	pJ/b	EIC Area (mm^2)	DSP
[1]	Wire-bonding (2D)	130nm BiCMOS	160	65	0.8	-7	0.99	0.82 ¹	5-tap FFE
[2]	Wire-bonding (2D)	55nm BiCMOS	224	57.3	0.89	-4.8	2.2	1.38 ¹	10-tap FFE
[3]	Flip-chip (3D)	N/A	160	N/A	0.85	-2.7	1.2	N/A	51-tap FFE
[4]	Flip-chip (3D)	16nm FinFET	106.25	77	N/A	-13.97	0.98	0.64	12-tap FFE + 1-tap DFE
[5]	Direct-bonding (3D)	130nm BiCMOS	264	60	0.9	N/A	1.45	0.6	6-tap FFE
[6]	Monolithic	45nm CMOS	112	68	0.245	N/A	1	N/A	N/A
This work	μ TP (3D)	130nm BiCMOS	224	53.6	0.9	-5.2	0.51	0.06	6-tap FFE

¹ data path core of one channel.

65 References

66 [1] Gu, Y., Lambrecht, J., Niu, S., Vandierendonck, A., Bruynsteen, C., Coudyzer,
67 G., De Bruyn, K., Bauwelinck, J., Yin, X., Ossieur, P.: A 160 Gb/s PAM-4 opti-
68 cal receiver using a fully differential transimpedance amplifier in SiGe BiCMOS.
69 Journal of Lightwave Technology **42**(23), 8237–8244 (2024)

70 [2] Declercq, J., Moeneclaey, B., Lambrecht, J., Bruynsteen, C., Singh, N., Niu, S.,
71 Ossieur, P., Yin, X.: A 64-GHz optical receiver for 128-GBd links using a 55-
72 nm SiGe BiCMOS traveling-wave linear transimpedance amplifier. Journal of
73 Lightwave Technology, 1–10 (2025)

74 [3] Wu, D., Wang, D., Chen, D., Yan, J., Dang, Z., Feng, J., Chen, S., Feng, P., Zhang,
75 H., Fu, Y., *et al.*: Experimental demonstration of a 160 Gbit/s 3D-integrated sili-
76 con photonics receiver with 1.2-pJ/bit power consumption. Optics Express **31**(3),
77 4129–4139 (2023)

78 [4] Lakshmikumar, K., Kurylak, A., Nandwana, R.K., Das, B., Pampanin, J.,
79 Brubaker, M., Hanumolu, P.K.: A 7 pA/ $\sqrt{\text{Hz}}$ asymmetric differential TIA for
80 100Gb/s PAM-4 links with -14dBm optical sensitivity in 16nm CMOS. In: 2023
81 IEEE International Solid-State Circuits Conference (ISSCC), pp. 206–208 (2023)

82 [5] Peczek, A., Wietstruck, M., Winzer, G., Mai, C., Lischke, S., Khafaji, M.M.,
83 Schulze, S., Voß, T., Krüger, P., Zimmermann, L.: 132 GBaud PAM4 IM/DD sil-
84 icon receiver subassembly realized by stacking technology. Journal of Lightwave
85 Technology, 1–6 (2025)

86 [6] Baehr-Jones, T., Ardalan, S., Chang, M., Jafarlou, S., Serey, X., Zarris, G., Thomp-
87 son, G., Darbinian, A., West, B., Behnia, B., Velev, V., Li, Y.Z., Roelofs, K., Wu,
88 W., Mali, J., Zhan, J., Ophir, N., Horng, C., Narevich, R., Guan, F., Yang, J.,
89 Wu, H., Maupin, P., Manley, R., Ahuja, Y., Novack, A., Wang, L., Streshinsky,
90 M.: Monolithically integrated 112 gbps pam4 optical transmitter and receiver in a
91 45nm cmos-silicon photonics process. Optics Express **31**(15), 24926–24938 (2023)